Photophysics, photochemistry, and reactivity: Molecular aspects of perylenequinone reactions

Rita Cardoso Guedes*[a] and Leif Axel Eriksson[b]

Received 2nd April 2007, Accepted 20th July 2007
First published as an Advance Article on the web 6th August 2007
DOI: 10.1039/b704869f

Density functional theory (DFT) and time-dependent density functional theory (TD-DFT) were used to elucidate the photochemistry and photophysics of eight different perylenequinones (PQ). The objective of this work has been to quantitatively investigate the photodynamic therapeutic potential of this family of compounds and give an overview of their photoreactivity. The effects of solvation were evaluated through single-point calculations using the integral equation formalism of the polarised continuum model. It is concluded that the eight studied perylenequinones can generate singlet oxygen (in aqueous solution) and superoxide radical anions, and that the autoionisation of two nearby PQ molecules is possible.

1. Introduction

Photodynamic therapy (PDT) and photophysical diagnosis (PPD) are innovative and non-invasive methods developed for treatment and detection of small and superficial tumours.[1,2]

In PDT a photosensitising drug is administered (and should accumulate selectively in tumour tissues), followed by light exposure/activation of a specific wavelength to generate cytotoxic reactive oxygen species (ROS)[3] produced during photoexcitation of the photosensitisers.[4] The results of PDT depend largely on the conditions under which it is carried out, such as the drug delivery to light exposure interval, light exposure regime, localisation and concentration of the photosensitiser, cell type, *etc.* As laser and optical techniques develop rapidly, PDT depends particularly on the development of new photosensitizers. A good photosensitizer should have a strong absorption in the phototherapeutic window (600–900 nm, where tissue light scattering is low and there is a modest competing absorption from haemoglobin, melanin and water), high quantum yield of triplet formation, high preferential tumour localization, minimal dark toxicity, and a fast clearance rate from the normal tissues.

More than 400 compounds are known to display photosensitizing properties including dyes, drugs, cosmetics, chemicals and many natural substances. The majority of these molecules used for medical purposes belong to the basic structures of tricyclic dyes with different meso-atoms, tetrapyrroles, or furocoumarins.

Most of the experimental and clinical data have been obtained with first generation photosensitizers, such as hematoporphyrin derivatives and its partially purified form, Photofrin II.[5,6] The porphyrins are an important class of compounds in biological systems because of their central role in photosynthesis, biological oxidation and reduction, and oxygen transport (the basic porphyrin skeleton comprises four pyrrole rings, conjugated together through four extra carbon atoms). However, the lack of therapeutic selectivity and the side effects (long-lasting normal tissue photosensitivity) limit their clinical use.[7] Intravesical administration of Photofrin has failed to photosensitise some tumours, such as bladder tumours that constitute the second most common genitourinary malignancy.[8] An estimate of 357 000 bladder cancer cases occurred in 2002 (with 145 000 deaths),[9] making this the ninth most common cause of cancer for both sexes combined. In this type of cancer, most patients (85%) have superficial disease at the time of initial diagnosis and there is strong evidence that perylenequinones are promising photodynamic therapeutic agents in these cases.[10]

Perylenequinones (PQ), or 4,9-dihydroxy-3,10-perylenequinones, are naturally occurring pigments that have attracted much interest during last decades due to their outstanding light-induced biological activity and their unique photophysical properties that render them new potential compounds to the use in PDT and PPD.[8] They present some advantages over hematoporphyrins in that they are easy to prepare and purify, they are facile towards site-directed chemical modifications, they have large molar absorptivity at the appropriate wavelength, good solubility, display small influence of the solvents on the photochemical reactions, large concentration tolerance, high thermal stability, high quantum yields of singlet oxygen, fast clearance from normal tissues,[11] and require oxygen for their antiviral activity.[12] PQs are an efficient class of ROS generators with quantum yields comparable with those of porphyrins. Former comparative studies have demonstrated that the 4,9-dihydroxy-3,10-perylenequinonoid chromophore is an essential structural requirement for the generation of ROS by the quinones, and that the side chains only had a little effect on this generation.[8]

In the constant strive to design, synthesise and characterise new photosensitizers that exhibit high efficiency and low dark toxicity, information from modern theoretical methods (*e.g.* absorption spectra, singlet–triplet energy gap, substituents effects, solvent effects, *etc.*) is very helpful and can be considered indispensable before synthesis and *in vitro* and *vivo* tests. Recently, computational studies have been carried out on other photosensitisers to elucidate their potentialities as active molecules in photodynamic therapy.[13–15]

[a]*iMED.UL/CECF, Faculty of Pharmacy of the University of Lisbon, Av., Prof. Gama Pinto 2, 1649-016, Lisbon, Portugal. E-mail: rguedes@ff.ul.pt*
[b]*Dept. of Natural Sciences and Örebro Life Science Center, Örebro University, Fakultetsgatan 1, 70182, Örebro, Sweden*

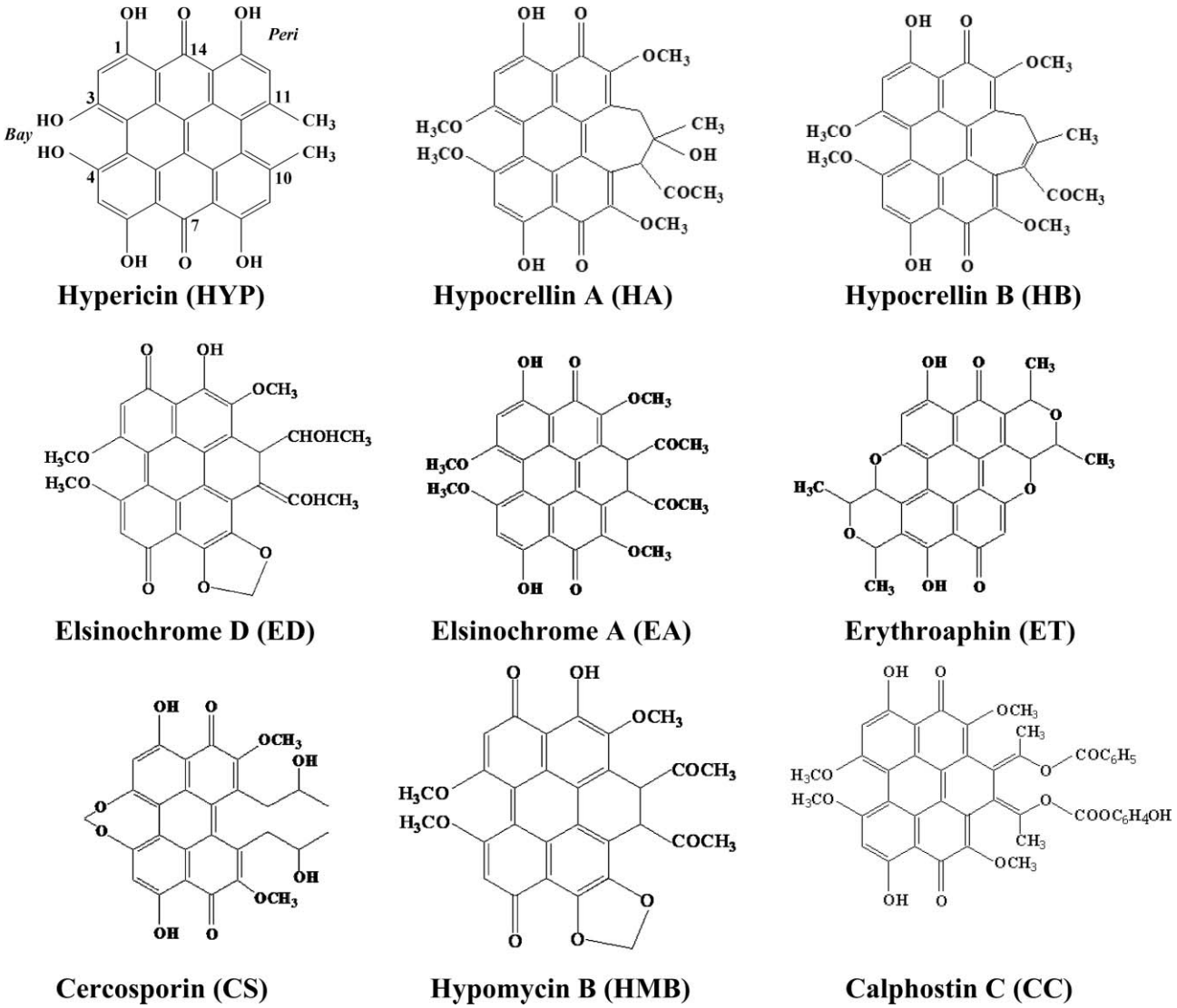

Fig. 1 Perylenequinones investigated in the present work.

The purpose of this paper is to quantitatively evaluate the photophysical and photochemical properties of perylenequinones (PQ) (Fig. 1) hypocrellin A (HA), hypocrellin B (HB), cercosporin (CS), elsinochrome A (EA), elsinochrome D (ED), erythroaphin (ET), calphostin C (CC), and hypomycin B (HMB) from theoretical quantum calculations based on density functional theory (DFT) and time-dependent density functional theory (TD-DFT).

In particular, we have determined the geometric structures, absorption spectra, singlet–triplet energy gap, ionisation potentials, electron affinities, solvent effects, and possibility of photosensitized reactions with molecular oxygen.

2. Theoretical approach

Prior to calculating excited states, all structures were geometry optimized without symmetry constraints using Becke's three-parameter hybrid functional method[16] (B3LYP) in conjunction with the 6-31G(d)[17] basis set. The minimum geometries were confirmed by harmonic vibrational frequency analysis. Data used for estimation of ionisation potentials (IPs), electron affinities (EAs) and excitation energies were calculated at the B3LYP/6-31G+(d,p)//B3LYP/6-31G(d) level of theory. The EA is defined as the energy required to add an electron to a neutral molecule, and calculated as the energy of the neutral molecule minus the energy of the anion. The reverse applies to the IP, which is the energy needed to remove electrons. In the calculation of the adiabatic EA and IP (AEA, AIP), the geometries of the neutral and the ionised molecules were fully optimised, whereas in the calculation of vertical EA and IP (VEA, VIP), the energies of the ionised molecules were calculated using the optimized structures of the neutral molecules. Vertical excitation energies, transition intensities and oscillator strengths were computed employing time-dependent[18] density functional theory (TD-DFT)[19–20] at the B3LYP/6-31+G(d,p) level using the optimised ground-state geometries. The use of diffuse functions has previously been shown to be critical for accurate determination of the energetics, particularly for anionic and excited states.[21] For excitations not involving charge transfer, TD-DFT in combination with the B3LYP hybrid

functional and the 6-31+G(d,p) basis set are known to generally provide energies to within ~0.2 eV (5 kcal mol^{-1}).[22] In the case of charge-transfer excitations, the accuracy is less—usually within 0.4 eV. Computed transitions furthermore tend to give too high, rather than too low, excitations energies compared with experimental data. For more detailed investigations of tends in computed excitation energies at the TD-DFT level, see, *e.g.*, ref. 23–25. Solvent effects were included through single-point calculations using the integral equation formalism of the polarisable continuum model (IEF-PCM)[26,27] of Tomasi and co-workers. Two different values for the dielectric constant were used, $\varepsilon = 4$ and $\varepsilon = 78$, corresponding to a hydrophobic environment and to bulk water. Previous work has shown that in the current formalism, bulk effects have a minor effect in the calculation of excitation energies,[28] and were thus not included in the TD-DFT calculations reported herein. All calculations were performed using the Gaussian03 package.[29]

3. Results and discussion

This section is organised in three different parts in which the geometries, the excitation energies, and the subsequent photosensitized reactions will be discussed.

3.1 Ground-state geometries

The ground state geometries of the eight perylenequinones and hypericin (Fig. 1), and their respective radical anions and radical cations were optimized and some key structural parameters (O–O, O–H, C=O, *etc.*) in the *peri* regions are presented in Table 1. The geometries of the perylenequinones molecules show (like hypericin) a slightly distorted structure defined by the two dihedral angles D_l(C3–C–C–C4) and D_r(C10–C–C–C11) (HYP nomenclature; Fig. 1), caused by repulsive interactions between the bay groups.

As can be seen from Table 1, the bond lengths do not change significantly within the perylenequinone family and when compared with hypericin. For example, the O–O distance on the top *peri* region (common to all the studied perylenequinones) is always between 2.583 and 2.506 Å (2.542 Å in HYP). The same applies to the top *peri* region O–H distance that is almost constant (between 1.010 and 1.016 Å, and 0.999 Å in HYP). The major change is found when we compare the C=O distances in HYP (1.350 and 1.377 Å) with the remaining perylenequinone family (between 1.232 and 1.265 Å).

Contrary to the situation for the bond distances, the dihedral angles change considerably. HA and HB show torsional angles close to the ones of HYP, but the dihedrals change a lot for the other studied compounds.

It is often useful to relate simple chemical descriptors to the excitation spectra. In Fig. 2 we show the correlation between the excitation spectra and the torsion D_r of the studied compounds. The larger the value of the dihedral angle D_r, the lower the excitation energy. However, as the different compounds also have different substitution patterns, the spread in the values is quite large. We also note that a clear correlation as that for D_r *vs.* E is not seen for D_l *vs.* E. The fact that the more distorted structures render lower excitation energies is due to the reduced HOMO → LUMO gap resulting from the strain (as we are still well within the range of a conjugated system).

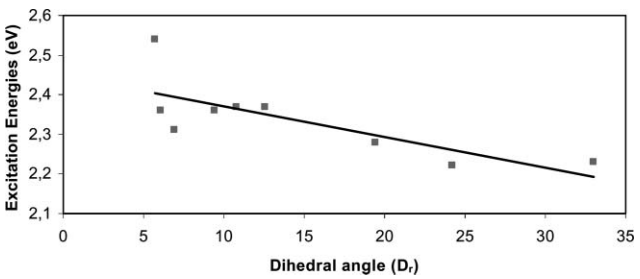

Fig. 2 Correlation between singlet excitation energy (eV) and dihedral angle D_r (°) of the studied perylenequinones.

3.2 Formation of excited states

As described earlier,[4,30] the photosensitized reactions are initiated by excitation to the short-lived first excited singlet state (S_0) → (S_1) followed by intersystem crossing to the first excited triplet

Table 1 Selected geometric parameters for the optimised structures of the perylenequinone compounds

	B3LYP/6-31G(d)								
	Distances/Å	HYP	HA	HB	CS	HMB	EA	ED	ET	CC
	O–O (t)[a]	2.542	2.506	2.532	2.525	2.538	2.534	2.525	2.583	2.537
	O–H (t)[a]	0.999	1.014	1.010	1.007	1.014	1.010	1.016	1.005	1.010
	H–O (t)[a]	1.638	1.571	1.604	1.608	1.604	1.607	1.585	1.665	1.610
	H–O (t)[a]	1.651	2.375	2.358	2.492	—	2.398	—	2.435	2.305
	C=O (t)[a]	1.350	1.265	1.263	1.257	1.259	1.261	1.261	1.258	1.261
	O–O (b)[a]	2.553	2.511	2.527	2.514	2.814	2.535	2.807	2.565	2.536
	O–H (b)[a]	0.971	1.015	1.012	1.008	—	1.010	—	1.012	1.010
	C=O (b)[a]	1.377	1.265	1.262	1.260	1.232	1.261	1.233	1.257	1.261
	H–O (b)[a]	1.660	2.244	2.377	2.393	—	2.241	—	—	2.280
	Dihedrals/°									
	D_l	25.8	33.4	32.5	7.4	25.4	29.5	25.5	7.3	29.7
	D_r	33.0	19.4	24.2	12.6	5.7	9.4	6.9	6.1	10.8

[a] (t): top *peri* region; (b): bottom *peri* region.

state (S_1) → (T_1) which results in more stable and (relatively) longer lived species. PQ compounds in general have three strong visible absorption bands (Ia, IIa, and IIIa), which are respectively assigned to a π–π* transition in the conjugated systems (Ia) and charge transfer (IIa and IIIa).[8] Diwu *et al.* showed in 1992[32] that there are no significant differences (<12 nm) between the HB, HA, and CS absorption spectra in various solvents at room temperature.

In Table 2 we report the vertical excitation energies, oscillator strengths, and transition character for the six lowest spin-allowed singlet transitions in vacuum of the series of perylenequinones, and compare with experimental data available in the literature. For comparison, previously reported hypericin data[31] have also been included in the table.

Analysing the data in the table, we note that the absorption spectra of all perylenequinones are between 370–560 nm, in the UV-Vis region. For the studied compounds the lowest excitation energy varies from 2.22 eV (HB) to 2.54 eV (HMB) with oscillator strengths (f) between 0.08 and 0.17. These transitions stem mainly from the HOMO → LUMO excitation, except for CS that shows HOMO-1 → LUMO excitation. The second lowest excitation energy falls between 2.28 eV (HB) and 2.87 eV (ET), with oscillator strengths $0.05 < f < 0.30$, and generally involves the HOMO-1 → LUMO transition as the main component. CS is again an exception, with lowest excitation arising from HOMO → LUMO and HOMO-3 → LUMO transitions, and is relatively strong (f = 0.30). The higher calculated excitations vary between 2.58 eV and 3.30 eV.

Within the perylenequinone family, HB and HA show the lowest lying excited singlet states, 2.22 (558 nm) and 2.28 eV (543 nm) respectively. Shen *et al.*[38] calculated (by a combined DFT method, B3LYP/6-31G(d,p)//B3LYP/6-31G) the five lowest singlet excitation energies and oscillator strengths for HA in benzene (528, 504, 453, 441, and 414 nm) and DMSO (526, 499, 461, 442, and 403 nm) solutions, values that are in close agreement with our gas phase results. Note that at 500 nm, a 50 nm shift (*e.g.* 500–550 nm) corresponds to an energy difference of only 0.23 eV. When we compare the first excitation energies of HB, and HA with the other perylenequinones, we conclude that the presence of a seven-membered ring decreases the excitation energy by at least 0.1 eV, red-shifting the excitations. Furthermore, the difference in the bay dihedral angles observed suggests that there is a correlation between the first singlet excitation energy and the perylenequinone skeleton torsional deformation. In general, the larger the torsional deformation (without breaking the conjugation) the more red-shifted the absorption.

The highest first excitation energy is found for CS (2.43 eV) and HMB (2.54 eV).

Only for CC does the first excited singlet state have the highest probability, whereas the second and third singlet excitations show the strongest probabilities for the other compounds. In general, the last two excitations calculated show very low probability.

Comparing the different excitation energies for the studied PQs and HYP, we conclude that only HB is more easily excited than HYP, suggesting that this molecule has the potential to initiate photosensitized reactions more readily.

Due to the efficient intersystem crossing (ISC) to the long-lived excited triplet states, these states often serve as a starting point for a wide range of photochemical processes. The computed lowest lying triplet excitation energies for the perylenequinones studied are listed in Table 3.

One of the basic requisites for a photosensitizer in achieving optimal performance in PDT is represented by its singlet → triplet energy gap. All the calculated first excited triplet states lie lower in energy than their corresponding first excited singlets. The calculated gap between the first excited singlet and first excited triplet state, $S_1 \rightarrow T_1$, is in the 0.6–1.0 eV (14–23 kcal mol^{-1}) range, in fair agreement with the experimental energy gap obtained by Diwu *et al.*[32] for HA, HB, and CS (0.38 eV; 7.5 kcal mol^{-1}). Two sources for the difference between experimental and theoretical data are the ~0.2 eV overestimated singlet excitation energies, and the lack of structural relaxation in the structures used for evaluation of the excited states. The first excited triplet states lies between 1.32 and 1.75 eV above the corresponding ground states. The lowest first excited triplet state (T_1) is found for HB, at 1.32 eV.

3.3 Oxygen-dependent type I reactions

Photochemical reactions are classified into two categories, oxygen-dependent and oxygen-independent (anoxic) processes. In oxygen-dependent type I reactions an electron donor (D) may readily reduce the sensitizer in the excited triplet state, with subsequent electron transfer to molecular oxygen and formation of reactive superoxide anions.

$$\mathrm{Sens}(T_1) + \mathrm{D} \rightarrow \mathrm{Sens}^{\bullet -} + \mathrm{D}^{\bullet +} \quad (1)$$

$$\mathrm{Sens}(S_0)^{\bullet -} + {}^3O_2 \rightarrow \mathrm{Sens}(S_0) + O_2^{\bullet -} \quad (2)$$

In Table 4 we list the computed ground state electron affinities of the studied perylenequinones in vacuum, in an hydrophobic environment, and in aqueous solution, as well as the energy gain when reducing the corresponding T_1 states.

The calculated vertical electron affinities lie in the energy range 1.7–3.7 eV, and the adiabatic ones in the energy range 2.1–3.9 eV. This shift by 0.2–0.4 eV arises due to the structural relaxation of the anion, giving higher AEA values. If the perylenequinones are first excited to the triplet state, T_1, the electron affinities increase to between 3.4–5.3 eV. VEA(T_1) is a measure of the energy gain upon reduction from the T_1 state; the larger the VEA(T_1), the easier it is for the compound to oxidise a nearby species (*e.g.* a DNA nucleobase). As expected, the oxidising power of the perylenequinones is enhanced in aqueous solution, due to the fact that the polar medium stabilizes the charged species. Among the different PQs erythroapin (ET) is the strongest oxidising agent from the excited triplet state, and hypocrellin B the weakest. The order is markedly different compared to the situation based on the ground state EAs. Another important piece of information is that several of the compounds studied (CS, HMB, EA, ED, ET and CC) are stronger oxidising agents in aqueous solution than HYP.

After reduction ($PQ^{\bullet -}$), the perylenequinones can undergo electron transfer to molecular oxygen ($^3O_2$), forming the reactive superoxide radical anion ($O_2^{\bullet -}$) and regenerating the neutral perylenequinones (PQ). Comparing the ground state adiabatic electron affinity of molecular oxygen in vacuum (0.59 eV[22]) and aqueous solution (3.91 eV[22]), with the corresponding ground state electron affinities of PQ we can predict whether this electron transfer reaction is feasible or not. The computed data suggest that

Table 2 Vertical singlet excitation energies in eV and nm, oscillator strengths, f, and transitions character (TC) computed at the B3LYP/6-31+G(d,p) level. Experimental data in parentheses

HYP[31]	E_{0-0}	2.23	2.76	2.86	3.08	3.19	3.35
	λ	556	450	433	402	388	370
	f	0.24	0.17	0.05	0.02	0.02	0.01
HA	E_{0-0}	2.28	2.40	2.74	2.83	3.01	3.10
	λ	543	516	452	437	411	400
		(583,[32] 575,[33] 541,[32] 536,[33] 471,[32] 461[33])					
	f	0.14	0.24	0.04	0.15	0.01	0.00
	TC	0.58(H → L)	−0.20(H-1 → L)	0.49(H-2 → L)	0.11(H-3 → L)	0.11(H-	−0.10(H-5 → L+1)
		−0.25(H-1 → L)	0.53(H-1 → L)	−0.45(H-3 → L)	−0.17(H-1 → L)	4 → L+1)	0.66(H-5 → L)
			0.27(H-2 → L)		0.38(H-2 → L)	0.67(H-4 → L)	−0.15(H-7 → L)
			−0.11(H → L)		0.50(H-3 → L)		
HB	E_{0-0}	2.22	2.28	2.62	2.78	2.93	3.03
	λ	558	544	474	446	423	409
		(580,[32]582,[34]540,[34]548,[32]466,[32]467[34])					
	f	0.11	0.14	0.25	0.05	0.01	0.01
	TC	0.51(H → L)	0.63(H-1 → L)	−0.31(H → L)	−0.12(H → L)	−0.29(H-3 → L)	−0.10(H-3 → L)
		0.41(H-2 → L)		0.52(H-2 → L)	0.64(H-3 → L)	0.53(H-4 → L)	0.43(H-4 → L)
				−0.19(H-3 → L)	0.14(H-4 → L)	−0.30(H-5 → L)	0.39(H-5 → L)
							0.24(H-6 → L)
							0.22(H-7 → L)
							0.11(H-8 → L)
CS	E_{0-0}	2.43	2.51	2.68	2.88	3.03	3.07
	λ	510	494	462	430	409	404
		(566,[32] 560, 524,[32] 476,[32] 470[35])					
	f	0.13	0.30	0.01	0.10	0.01	0.01
		0.64(H-1 → L)	0.58(H → L)	0.67(H-2 → L)	−0.18(H → L)	0.50(H-4 → L)	−0.12(H-4 → L)
			0.21(H-3 → L)		0.64(H-3 → L)	0.29(H-5 → L)	0.10(H-5 → L + 1)
						0.36(H-6 → L)	0.59(H-5 → L)
							−0.32(H-6 → L)
HMB	E_{0-0}	2.54	2.77	2.82	2.92	3.09	3.29
	λ	488	448	440	425	401	377
		(525,[36]524,[37]460,[36]456[37])					
	f	0.14	0.05	0.21	0.07	0.05	0.01
	TC	0.64(H → L)	−0.26(H-1 → L)	0.10(H → L + 3)	−0.20(H-1 → L)	0.13(H-1 → L)	−0.17(H-5 → L)
			0.16(H-2 → L)	0.51(H-1 → L)	0.55(H-2 → L)	−0.10(H-2 → L)	−0.12(H-6 → L + 1)
			0.45(H-3 → L)	0.35(H-2 → L)	−0.32(H-3 → L)	−0.33(H-3 → L)	0.60(H-6 → L)
			0.38(H-4 → L)	0.20(H-3 → L)		0.55(H-4 → L)	0.25(H-7 → L)
						0.12(H-8 → L)	
EA	E_{0-0}	2.36	2.45	2.68	2.86	2.96	3.10
	λ	525	507	462	433	419	400
		(568, 528, 459[32])					
	f	0.15	0.14	0.15	0.11	0.02	0.02
	TC	0.61(H-L)	0.15(H → L)	0.27(H-1 → L)	−0.20(H-1 → L)	0.12(H-2 → L)	0.15(H-5 → L)
		−0.16(H-1-L)	0.50(H-1 → L)	0.54(H-2 → L)	−0.11(H-2 → L)	0.62(H-4 → L)	0.12(H-6 → L)
			−0.38(H-2 → L)	0.25(H-3 → L)	0.62(H-3 → L)	−0.12(H-6 → L)	0.58(H-7 → L + 1)
			0.14(H-3 → L)	−0.10(H-4 → L)		−0.20(H-7 → L)	0.31(H-7 → L)
ED	E_{0-0}	2.31	2.54	2.73	2.89	3.08	3.30
	λ	536	488	454	430	402	375
	f	0.08	0.13	0.04	0.26	0.02	0.01
	TC	0.64(H → L)	0.63(H-1 → L)	0.28(H-2 → L)	0.16(H → L)	0.67(H-3 → L)	−0.11(H → L + 1)
		−0.24(H-2 → L)	−0.13(H-2 → L)	0.13(H-3 → L + 1)	0.10(H-1 → L)		0.47(H-4 → L)
				0.59(H-3 → L)	0.53(H-2 → L)		−0.21(H-5 → L)
					−0.30(H-3 → L)		−0.43(H-6 → L)
ET	E_{0-0}	2.37	2.87	2.89	2.99	3.08	3.09
	λ	522	432	430	415	403	401
	f	0.16	0.10	0.25	0.08	0.00	0.01
	TC	0.64(H → L)	0.34(H-1 → L)	0.47(H-1 → L)	−0.20(H-1 → L)	0.21(H-3 → L)	0.36(H-3 → L)
			0.57(H-2 → L)	−0.34(H-2 → L)	0.14(H-2 → L)	0.29(H-4 → L)	0.43(H-4 → L)
				0.17(H-3 → L)	0.51(H-3 → L)	0.57(H-5 → L)	−0.36(H-5 → L)
				−0.23(H-4 → L)	−0.34(H-4 → L)	0.10(H-7 → L)	
					−0.11(H-8 → L)		
CC	E_{0-0}	2.37	2.50	2.58	2.80	2.90	3.08
	λ	524	496	481	443	428	402
	f	0.17	0.11	0.09	0.15	0.01	0.03
	TC	0.63(H → L)	0.45(H-1 → L)	−0.31(H-1 → L)	−0.28(H-1 → L)	−0.18(H-2 → L)	−0.14(H-5 → L)
		−0.10(H-2 → L)	0.40(H-2 → L)	0.52(H-2 → L)	0.15(H-2 → L)	0.67(H-3 → L)	0.63(H-6 → L)
			0.12(H-3 → L)	0.11(H-3 → L)	0.57(H-3 → L)	−0.13(H-4 → L)	0.13(H-7 → L + 1)
			0.23(H-4 → L)	−0.27(H-4 → L)	−0.12(H-5 → L)		

Table 3 Vertical triplet excited state energies (in eV and nm) computed at the B3LYP/6-31+G(d,p) level

HYP[31]	E_{0-0}	1.62	2.03	2.26	2.53	2.76	2.97
	λ	765	611	548	491	449	418
HA	E_{0-0}	1.50	1.59	2.24	2.42	2.77	2.87
	λ	828	779	554	512	447	432
HB	E_{0-0}	1.32	1.51	2.09	2.36	2.68	2.72
	λ	940	821	594	524	462	456
CS	E_{0-0}	1.43	1.68	2.28	2.44	2.80	2.83
	λ	864	736	545	509	443	438
HMB	E_{0-0}	1.75	1.89	2.46	2.51	2.57	2.74
	λ	709	657	505	494	482	452
EA	E_{0-0}	1.50	1.59	2.24	2.42	2.77	2.87
	λ	828	779	554	512	447	432
ED	E_{0-0}	1.67	1.84	2.19	2.47	2.60	2.66
	λ	744	675	567	502	478	466
ET	E_{0-0}	1.62	1.77	2.39	2.60	2.80	2.86
	λ	767	699	518	476	443	434
CC	E_{0-0}	1.53	1.61	2.21	2.33	2.80	2.84
	λ	812	769	561	531	443	437

Table 4 Vertical and adiabatic electron affinities (VAE, AEA; in eV) in different media. $VEA(T_1) = VEA(S_0) + {}^3E_{0-0}$

	$VEA(T_1)$			VEA			AEA		
Medium	$\varepsilon = 1$	$\varepsilon = 4$	$\varepsilon = 78$	$\varepsilon = 1$	$\varepsilon = 4$	$\varepsilon = 78$	$\varepsilon = 1$	$\varepsilon = 4$	$\varepsilon = 78$
HYP	3.78	4.71	4.99	2.16	3.09	3.37	2.31	3.24	3.52
HA	3.40	4.52	4.92	2.05	3.16	3.56	2.41	3.49	3.81
HB	3.41	4.51	4.91	2.09	3.20	3.59	2.30	3.42	3.81
CS	3.84	4.81	5.07	2.41	3.38	3.64	2.65	3.63	3.91
HMB	3.65	4.78	5.17	1.90	3.03	3.42	2.12	3.23	3.61
EA	3.72	4.77	5.10	2.23	3.28	3.60	2.43	3.48	3.81
ED	3.39	4.58	5.02	1.73	2.91	3.35	2.25	3.27	3.58
ET	4.03	5.00	5.28	2.41	3.38	3.66	2.58	3.56	3.83
CC	3.57	4.66	5.08	2.04	3.14	3.56	2.26	3.34	3.73

once reduced, $PQ^{\bullet -}$ can indeed transfer an electron to molecular oxygen in aqueous solution, albeit all systems are far weaker reducing agents than hypericin (*cf.* AEA column in Table 4). We also note that for cercosporin (CS) the electron transfer reaction is thermoneutral, and hence less likely to proceed. In gas phase, the electron transfer is always energy forbidden.

3.4 Oxygen-dependent type II reactions

Photosensitizer mediated generation of singlet oxygen is highly favoured in nature, since energy-transfer reactions quenching both excited singlet and triplet states are spin-allowed. In oxygen-dependent type II reactions, the excitation energy of the sensitizer in its first excited triplet state is transferred to molecular oxygen to generate singlet molecular oxygen, a highly reactive species that despite its short half-life (4 μs in water), exerts strong cytotoxic effects, destroying cellular constituents such as nucleic acids, proteins, and unsaturated lipids.[39]

$$Sens(T_1) + {}^3O_2 \rightarrow Sens(S_0) + {}^1O_2 \quad (3)$$

Molecular oxygen is a ground state triplet possessing two very low-lying singlet states ($^1\Delta$ and $^1\Sigma$), with excitation energies 1.1 and 1.7 eV, respectively.[22] Since all the PQ compounds investigated herein have calculated T_1 states lying more than 1.3 eV above the ground state (*cf.* Table 3), we conclude that all PQs (independent of medium) can exert oxygen-dependent type II reactions, and hence serve as a source for the generation of ($^1\Delta$) singlet oxygen.

3.5 Direct electron transfer to O_2

Photooxidation is another photochemical reaction type proposed for the perylenequinones. This mechanism involves photoionization of the sensitizer coupled to electron uptake by molecular oxygen.

$$Sens(S_0 \text{ or } T_1) + {}^3O_2 \rightarrow Sens^{\bullet +} + O_2^{\bullet -} \quad (4)$$

To elucidate the possible occurrence of this reaction type it is necessary to compare the PQ ionization potentials with the electron affinities of ground state molecular oxygen. In Table 5 we list the ionization potentials for the studied PQ systems.

Table 5 Vertical and adiabatic ionisation potentials (VIP, AIP; in eV) in different media. $VIP(T_1) = VIP(S_0) - {}^3E_{0\text{–}0}$

	$VIP(T_1)$			VIP			AIP		
Medium	$\varepsilon = 1$	$\varepsilon = 4$	$\varepsilon = 78$	$\varepsilon = 1$	$\varepsilon = 4$	$\varepsilon = 78$	$\varepsilon = 1$	$\varepsilon = 4$	$\varepsilon = 78$
HYP	5.45	4.34	3.98	7.07	5.96	5.60	6.95	5.86	5.50
HA	5.69	4.77	4.46	7.04	6.13	5.81	6.57	5.69	5.46
HB	5.72	4.80	4.49	7.03	6.12	5.81	6.53	5.66	5.38
CS	6.10	5.01	4.57	7.54	6.44	6.00	6.97	5.82	5.40
HMB	5.53	4.44	4.14	7.28	6.19	5.89	7.10	6.19	5.89
EA	5.85	4.85	4.46	7.35	6.35	5.96	6.95	6.06	5.77
ED	5.22	4.30	3.98	6.89	5.97	5.65	6.66	5.75	5.47
ET	6.01	4.85	4.41	7.63	6.47	6.03	7.48	6.34	5.91
CC	5.52	4.70	4.39	7.05	6.22	5.92	6.63	5.89	5.66

The calculated adiabatic ionization potentials lie between 5.4 and 7.5 eV and the vertical ionization potentials between 5.6 and 7.6 eV. The difference between AIP and VIP is a measure of the geometry relaxation of the cation; the larger the difference, the bigger the change in the compound structure induced by the ionization. For the PQs studied, we found energy differences between 0.1 and 0.6 eV, and always larger than the one obtained for HYP. This reflects the increased torsion of the PQ skeleton upon ionization. The inclusion of the solvent reduces the ionization potential by about 1–1.6 eV, facilitating the PQ ionization. HYP and ED have the lowest IPs throughout, whereas the hypocrellins, CS and ET are the most difficult ones if considering the vertical IPs. Also allowing for structural relaxation (AIP), ED and the two hypocrellins are now the easiest to ionize, whereas ET and HMB are the most difficult ones. This reflects the different extent of structural relaxation for the different species. Comparing the ionization potentials of the PQs with the electron affinity of molecular oxygen in aqueous solution (3.91 eV) is obvious that O_2 is not capable of ionizing any of the PQs. Also the excited PQs have too high ionization potentials (column $VIP(T_1)$) to be oxidized by molecular oxygen; lowest IP in aqueous solution being 3.98 eV (HYP and ED). However, once sufficient energy is provided to eject an electron from the PQs it may be readily captured by molecular oxygen.

3.6 Disproportionation

Finally, we consider the possibility of two PQs being able to undergo disproportionation reactions. That is, once a sensitizer is excited to the triplet state, either the excited triplet molecule can be reduced by another PQ molecule in its ground state, or, alternatively, an excited triplet state PQ molecule can reduce another PQ molecule in the excited triplet state located in the nearby surrounding.

To analyse the possibility of these reactions to occur we need to consider the gain in energy when the $PQ(T_1)$ states are reduced. We see from Table 4 that the energy gain upon reduction of $PQ(T_1)$ in aqueous solution is between 3.4 and 5.3 eV, and from Table 5 that of $PQ(S_0)$ VIPs are between 5.6 and 7.6 eV. This implies that the triplet state cannot be reduced by a ground state PQ neither in gas phase nor in solution. However, in aqueous solution it is, for all systems explored, possible that disproportionation can occur between molecules in their first excited triplet states. ($VEA(T_1)$ 4.9–5.3 eV; $VIP(T_1)$ 4.0–4.6 eV).

4. Conclusions

By means of DFT and TD-DFT tools we have investigated the photo-physicochemical properties of eight perylenequinones including excitation energies, vertical and adiabatic electron affinities and ionization potentials, in vacuum, and in hydrophobic and aqueous environment. Our results can be summarised as follows:

(1) our methodology can correctly reproduce (within ~0.2 eV) and predict singlet and triplet excitation energies. The main transitions come from the HOMO → LUMO excitations with only small contributions from other neighbouring occupied molecular orbitals;

(2) the presence of the hypocrellin seven-membered ring red shifts the main absorption energy;

(3) the energy gap (singlet → triplet) of the studied PQ is between 0.6 and 1.0 eV;

(4) after excitation and depending on medium PQs can react by oxygen-dependent type I and type II reactions;

(5) excited PQs can not transfer an electron directly to oxygen;

(6) the autoionisation of two nearby excited PQ molecules is possible.

We have demonstrated that PQ can undergo oxygen-dependent type I and type II reactions. These reactions are favoured depending on the medium. In the presence of appropriate electron donors, the PQ is probably reduced and its extra electron is transferred to molecular oxygen generating superoxide radical anion. However, all the PQs studied are weaker reducing agents than HYP and consequently a weaker source of superoxide radical anions. In the absence of electron donors the PQs are able to transfer the excitation energy from the T_1 state to molecular oxygen, being in that way a source of singlet oxygen. HMB and the two elsinochromes have the highest T_1 energies (higher than HYP), and a similar carbon skeleton. These may hence pose promising candidates for new PDT compounds, especially if combined with structural features inducing large torsions in the 'D_r' region. More studies in this direction are currently being conducted.

Acknowledgements

R.C.G. thanks Fundação para a Ciência e a Tecnologia for financial support through a post-doctoral grant (SFRH/BPD/11501/2002). The Swedish Science Research Council (VR) and Sparbanksstiftelsen Nya are also acknowledged for financial support (L.A.E.). We furthermore acknowledge

grants of computing time at the supercomputing facilities in Linköping (NSC).

References

1 R. L. Lipson and E. J. Baldes, The photodynamic properties of a particular hematoporphyrin derivative, *Arch. Dermatol.*, 1960, **82**, 508–516.
2 R. Bonnett, Chemical aspects in photodynamic Therapy - (Advanced chemistry texts), Gordon and Breach Science Publishers, Amsterdam, 2000, vol. 1.
3 D. E. Dolmans, D. Fukumura and R. K. Jain, Photodynamic therapy for cancer, *Nat. Rev. Cancer*, 2003, **3**, 380–387.
4 K. Szacilowski, W. Macyk, A. Drzewiecka-Matuszek, M. Brindell, G. Stochel and Bioinorganic, Photochemistry: Frontiers and Mechanisms, *Chem. Rev.*, 2005, **105**, 2647–2694.
5 J. Moan, On the diffusion length of singlet oxygen in cells and tissues, *J. Photochem. Photobiol., B*, 1990, **5**, 521–524.
6 T. J. Dougherty, Photodynamic therapy (PDT) of malignant-tumors, *CRC Crit. Rev. Oncol. Hematol.*, 1984, **2**, 83–116.
7 J. S. McCaughan, Jr., Overview of experiences with photodynamic therapy for malignancy in 192 patients, *Photochem. Photobiol.*, 1987, **46**, 903–909.
8 J. W. Lown, 1976 Hoffman-LaRoche Award Lecture Photochemistry and photobiology of perylenequinones, *Can. J. Chem.*, 1997, **75**, 99–119.
9 D. M. Parkin, F. Bray, J. Ferlay, P. Pisani and Global, Cancer statistics 2002, *CA Cancer J. Clin.*, 2005, **55**, 74–108.
10 R. Y. Liang, G. D. Mei and W. Y. Zhou, 62 cases with hypertrophic scars treated with hypocrellin photochemothrapy, *Chin. J. Denna*, 1982, **15**, 87–88.
11 Z. Diwu, Novel therapeutic and diagnostic applications of hypocrellins and hypericins, *Photochem. Photobiol.*, 1995, **61**, 529–539.
12 J. Park, D. S. English, Y. Wannemuehler, S. Carpenter and J. W. Petrich, The role of oxygen in the antiviral activity of hypericin and hypocrellin, *Photochem. Photobiol.*, 1998, **68**, 593–597.
13 A. Domenico, N. Russo and E. Sicília, Structures and electronic absorption spectra of a recently synthesised class of photodynamic therapy agents, *Chem.–Eur. J.*, 2006, **12**, 6797–6803.
14 L. Petit, C. Adamo and N. Russo, Absorption spectra of first-row transition metal complexes of bacteriochlorins: a theoretical analysis, *J. Phys. Chem. B*, 2005, **109**, 12214–12221.
15 L. Petit, A. Quartarolo, C. Adamo and Nino Russo, Spectroscopic properties of porphyrin-like photosensitisers: insights from theory, *J. Phys. Chem. B*, 2006, **110**, 2398–2404.
16 A. D. Becke, Density-functional thermochemistry. 3. The role of exact exchange, *J. Chem. Phys.*, 1993, **98**, 5648–5652.
17 R. Ditchfield, W. J. Hehre and J. A. Pople, Self-consistent molecular-orbital methods. 9. Extended gaussian-type basis for molecular-orbital studies of organic molecules, *J. Chem. Phys.*, 1971, **54**, 724–728.
18 M. E. Casida, in *Recent Advances in density functional methods, part 1*, ed. D. P. Chong, World Scientific, Singapore, 1995.
19 R. E. Stratmann, G. E. Scuseria and M. J. Frisch, An efficient implementation of time-dependent density-functional theory for the calculation of excitation energies of large molecules, *J. Chem. Phys.*, 1998, **109**, 8218–8224.
20 M. E. Casida, C. Jamorski, K. C. Casida and D. R. Salahub, Molecular excitation energies to high-lying bound states from time-dependent density-functional response theory: Characterization and correction of the time-dependent local density approximation ionization threshold, *J. Chem. Phys.*, 1998, **108**, 4439–4449.
21 S. D. Wetmore, L. A. Eriksson and R. J. Boyd, in *Theoretical and Computational Chemistry, Theoretical Biochemistry - Processes and Properties of Biological Systems*, ed. L. A. Eriksson, Elsevier, Amsterdam, 2001, vol. 9.
22 J. Llano and L. A. Eriksson, First principles electrochemical study of redox events in DNA bases and chemical repair in aqueous solution, *Phys. Chem. Chem. Phys.*, 2004, **6**, 2426–2433.
23 S. Grimme and M. Parac, Substantial errors from time-dependent density functional theory for the calculation of excited states of large π-systems, *ChemPhysChem*, 2003, **4**, 292–295.
24 P. Homem-de-Mello, B. Mennucci, J. Tomasi and A. B. F. da Silva, The effects of solvation in the theoretical spectra of cationic dyes, *Theor. Chem. Acc.*, 2005, **113**, 274–280.
25 M. Guillaume and B. Champagne, F. Z Investigation of the UV/Visible absorption spectra of merocyanine dyes using time-dependent density functional theory, *J. Phys. Chem. A*, 2006, **110**, 13007–13013.
26 B. Mennucci, R. Cammi and J. Tomasi, Excited states and solvatochromic shifts within a nonequilibrium solvation approach: A new formulation of the integral equation formalism method at the self-consistent field, configuration interaction, and multiconfiguration self-consistent field level, *J. Phys. Chem.*, 1998, **109**, 2798–2807.
27 D. M. Chipman, Reaction field treatment of charge penetration, *J. Chem. Phys.*, 2000, **112**, 5558–5565; E. Cancès and B. Mennucci, Comment on "Reaction field treatment of charge penetration", *J. Chem. Phys.*, 2001, **114**, 4744–4745.
28 J. Llano and L. A. Eriksson, Theoretical study of phototoxic reactions of psoralens, *J. Photochem. Photobiol., A*, 2003, **154**, 235–243.
29 M. J. Frisch, G. W. Trucks, H. B. Schlegel, G. E. Scuseria, M. A. Robb, J. R. Cheeseman, V. G. Zakrzewski, J. A. Montgomery, Jr., R. E. Stratmann, J. C. Burant, S. Dapprich, J. M. Millam, A. D. Daniels, K. N. Kudin, M. C. Strain, O. Farkas, J. Tomasi, V. Barone, M. Cossi, R. Cammi, B. Mennucci, C. Pomelli, C. Adamo, S. Clifford, J. Ochterski, G. A. Petersson, P. Y. Ayala, Q. Cui, K. Morokuma, D. K. Malick, A. D. Rabuck, K. Raghavachari, J. B. Foresman, J. Cioslowski, J. V. Ortiz, A. G. Baboul, B. B. Stefanov, G. Liu, A. Liashenko, P. Piskorz, I. Komaromi, R. Gomperts, R. L. Martin, D. J. Fox, T. Keith, M. A. Al-Laham, C. Y. Peng, A. Nanayakkara, C. Gonzalez, M. Challacombe, P. M. W. Gill, B. G. Johnson, W. Chen, M. W. Wong, J. L. Andres, M. Head-Gordon, E. S. Replogle and J. A. Pople, *GAUSSIAN 98 (Revision A.3)*, Gaussian, Inc., Pittsburgh, PA, 2003.
30 R. C. Guedes, L. A. Eriksson and Theoretical, characterization of aflatoxins and their phototoxic reactions, *Chem. Phys. Lett.*, 2006, **422**, 328–333.
31 R. C. Guedes and L. A. Eriksson, Theoretical study of hypericin, *J. Photochem. Photobiol., A*, 2005, **172**, 293–299.
32 Z. J. Diwu and J. W. Lown, Photosensitization by anticancer agents. 12. Perylene quinonoid pigments, a novel type of singlet oxygen sensitizer, *J. Photochem. Photobiol., A*, 1992, **64**, 273–287.
33 L. Ma, H. Tai, C. Li, Y. Zhang, Z.-H Wang and W.-Z. Ji, Photodynamic inhibitory effects of three perylenequinones on human colorectal carcinoma cell line and primate embryonic stem cell line, *World J. Gastroenterol.*, 2003, **9**, 485–490.
34 L. Li, Y. Chen, J. Shen, M. Zhang and T. Shen, New long-wavelength perylenequinones: synthesis and phototoxicity of hypocrellin B derivatives, *Biochim. Biophys. Acta*, 2000, **1523**, 6–12.
35 M. E. Daub, M. Li, P. Bilski and C. F. Chignell, Dihydrocercosporin singlet oxygen production and subcellular localization: A possible defense against cercosporin phototoxicityin Cercospora, *Photochem. Photobiol.*, 2000, **71**, 135–140.
36 P. K. Chowdhury, K. Das, A. Datta, W.-Z. Liu, H.-Y. Zhang and J. W. Petrich, A comparison of the excited-state processes of nearly symmetrical perylene quinones: hypocrellin A and hypomycin B, *J. Photochem. Photobiol., A*, 2002, **154**, 107–116.
37 H.-Y. Zhang, W. Liu, W.-Z. Liu and J.-L. Xie, Photosensitization of hypomycin B-A novel perylenequinonoid pigment with only one intramolecular hydrogen bond, *Photochem. Photobiol.*, 2001, **74**, 191–195.
38 L. Shen, H.-F. Ji, H.-Y Zhang and A TD-, DFT study on photophysicochemical properties of hypocrellin A and its implications for elucidating the photosensitizing mechanisms of the pigment, *J. Photochem. Photobiol., A*, 2006, **180**, 65–68.
39 N. Kitamura, S. Kohtani and R. Nakagaki, Molecular aspects of furocoumarin reactions: Photophysics, photochemistry, photobiology, and structural analysis, *J. Photochem. Photobiol., C*, 2005, **6**, 168–185.

